0013-7227/00/$03.00/0
Endocrinology

Vol. 141, No. 1
Printed in U.S.A.

Genetic Targeting of Green Fluorescent Protein to Gonadotropin-Releasing Hormone Neurons: Characterization of Whole-Cell Electrophysiological Properties and Morphology*

KELLY J. SUTER, WALTER J. SONG, TRACI L. SAMPSON, JEAN-PIERRE WUARIN, JUSTIN T. SAUNDERS, F. EDWARD DUDEK, AND SUZANNE M. MOENTER

Department of Anatomy and Neurobiology (K.J.S., T.L.S., J.-P.W., F.E.D.), Animal Reproduction and Biotechnology Laboratory (K.J.S.), Colorado State University, Fort Collins, Colorado 80523; and Departments of Internal Medicine and Cell Biology (W.J.S., J.T.S., S.M.M.), National Science Foundation Center for Biological Timing, University of Virginia, Charlottesville, Virginia 22908

ABSTRACT

GnRH neurons form the final common pathway for central control of reproduction, with regulation achieved by changing the pattern of GnRH pulses. To help elucidate the neurobiological mechanisms underlying pulsatile GnRH release, we generated transgenic mice in which the green fluorescent protein (GFP) reporter was genetically targeted to GnRH neurons. The expression of GFP allowed identification of 84–94% of immunofluorescently-detected GnRH neurons. Conversely, over 99.5% of GFP-expressing neurons contained immunologically detectable GnRH peptide. In hypothalamic slices, GnRH neurons could be visualized with fluorescence, allowing for identification of individual GnRH neurons for patch-clamp recording and subsequent morphological analysis. Whole-cell current-clamp recordings revealed that all GnRH neurons studied (n = 23) fire spontaneous action potentials. Both spontaneous firing (n = 9) and action potentials induced by injection of depolarizing current (n = 17) were eliminated by tetrodotoxin, indicating that voltage-dependent sodium channels are involved in generating action potentials in these cells. Direct intracellular morphological assessment of GnRH dendritic morphology revealed GnRH neurons have slightly more extensive dendrites than previously reported. GnRH-GFP transgenic mice represent a new model for the study of GnRH neuron structure and function, and their use should greatly increase our understanding of this important neuroendocrine system. (*Endocrinology* **141:** 412–419, 2000)

THE NEURONS THAT synthesize and secrete GnRH form the final common pathway for the central regulation of reproduction. GnRH stimulates the anterior pituitary to secrete the gonadotropic hormones LH and FSH, which subsequently induce gametogenesis and steroidogenesis. The pattern of GnRH in hypophyseal portal blood en route to the pituitary is strictly episodic (1–5); the sole known exception is the time of the preovulatory gonadotropin surge in the female, when levels of the decapeptide are continuously elevated for several hours (2, 5). The frequency and amplitude of GnRH release are altered in response to numerous factors, including steroid hormone feedback (2, 5), stress (6), nutrition (7, 8), and photoperiod (9, 10). It is through changing the frequency of GnRH release that these inputs alter reproductive status both physiologically and pathologically.

Despite the importance of modulations in GnRH-pulse characteristics to normal reproductive function, little is known about the cellular and molecular mechanisms underlying episodic GnRH release. Study of these neurons has been hampered by their rarity (600–2500 in the mammalian brain) and by their scattered distribution from the diagonal band of Broca through the medial basal hypothalamus (11). These factors have made isolation and/or identification of living GnRH neurons nearly impossible. To facilitate the study of living GnRH neurons, we generated transgenic mice in which the jellyfish reporter, green fluorescent protein (GFP, 12–14), is genetically targeted to GnRH neurons. We report here the initial characterization of this mouse model, with regard to fidelity of transgene expression, morphological assessment of intracellularly labeled GnRH neurons, and basic electrophysiological properties of these neurons.

Received July 28, 1999.

Address all correspondence and requests for reprints to: Suzanne M. Moenter, Department of Medicine, Box 578 HSC, University of Virginia, Charlottesville, Virginia 22908. E-mail: smm4n@virginia.edu.

* This research was supported by National Institute of Child Health and Human Development/NIH through cooperative agreement (U54 HD-28934) as part of the Specialized Cooperative Centers Program in Reproduction Research and by NIH HD-34860 (to S.M.M.), The NSF Center for Biological Timing, NSFDIR 8920162 to Dr. Gene Block, NS-10355 (to K.J.S.), AFOSR and MH-59995 (to F.E.D.), and Animal Reproduction and Biotechnology Laboratory (HD-07031).

Materials and Methods

Transgene

A portion of the mouse GnRH promoter (−3446 to +23, generously provided by Dr. James Roberts, Mount Sinai School of Medicine, New York, NY) was used to drive expression of a transgene consisting of the B intron of rabbit β-globin (600 bp) as a splice donor/acceptor, the coding sequence for enhanced GFP (CLONTECH Laboratories, Inc., Palo Alto, CA; 739 bp) and the polyadenylation signal from human GH (627 bp). The transgene was excised from the plasmid by flanking restriction enzymes, gel purified, resuspended in sterile 10 mM Tris (pH 7.4) containing 0.25 mM EDTA, purified on an Elutip-D column

(Schleicher and Schuell, Inc., Keene, NH), and the concentration adjusted to 2–5 ng/μl in the same buffer for injection.

Animals

Mice were maintained on a 14-h light, 10-h dark photoperiod with *ad lib* access to standard chow (Harlan 7012, Bartonsville, IL) diet and water. Transgenic mice were generated through standard pronuclear injection of fertilized ova obtained from CBB6/F1 females (15). Transgenic offspring were identified through Southern dot blot analysis of DNA harvested from tail snips using a ^{32}P-labeled GFP probe. All procedures were carried out in accordance with the Animal Care and Use Committees of the University of Virginia and Colorado State University.

Immunofluorescence and immunocytochemistry

To determine the pattern of transgene expression, six F1 male and female mice (age, 21–60 days) were anesthetized with sodium pentobarbital (0.1–0.2 mg ip) and perfused through the left ventricle with 10 ml 0.1 M PBS (pH 7.4) containing 0.1% wt/vol $NaNO_3$, followed by 40 ml 4% paraformaldehyde in the same buffer. Brains were removed and postfixed in the same fixative 6–18 h, then infiltrated with 30% sucrose in PBS with 0.1% NaN_3 for cryoprotection. Coronal sections (40 μm) were cut on a cryostat from the base of the olfactory bulbs through the caudal extent of the mammillary bodies. Every sixth section was subjected to immunodetection to locate GnRH peptide using slight modifications of a previously described procedure (16). All reagents were diluted in PBS (pH7.4) containing 0.4–1.0% vol/vol Triton X-100. Sections were blocked 1 h at room temperature in 4% vol/vol normal donkey serum (Jackson ImmunoResearch Laboratories, Inc., West Grove, PA), then incubated with LR1 anti-GnRH antibody (a generous gift of Dr. Robert Benoit, McGill University, 1:20,000 in block, 48–96 h, 4 C). Sections were then incubated in biotinylated donkey antirabbit IgG (1:200, 1 h, Jackson ImmunoResearch Laboratories, Inc.) followed by avidin-Texas red (1:100, 1 h, Vector Laboratories, Inc., Burlingame, CA). Sections were viewed with a Nikon (Garden City, NY) Microphot SA with epifluorescence to determine overlap of GFP signal with GnRH immunoreactivity. Images were captured with a Hamamatsu CCD camera and Open Lab software. For morphology, additional sections were prepared as above, with GnRH visualized by standard avidin-biotin-horseradish peroxidase complex using nickel-enhanced diaminobenzidine (Vector Laboratories, Inc.) as the chromogen.

Slices (200 μm) from electrophysiological work and control nonrecorded slices were fixed with 4% paraformaldehyde overnight. Recorded slices were incubated with strepavidin-Cy3 (1:1,000, Jackson ImmunoResearch Laboratories, Inc.) overnight at 4 C to confirm the identity of recorded cells. Immunodetection of GnRH was performed using the procedure detailed above, with an overnight extension of secondary antibody and avidin-biotin-horseradish peroxidase complex incubation at 4 C. For fluorescence detection of GnRH in recorded sections, Cy5 conjugated secondary antibody (1:200, Jackson ImmunoResearch Laboratories, Inc.) was used. For morphology, peroxidase detection was performed as described above.

Morphological analyses

Morphological analysis was performed on dendrites defined by immunoperoxidase labeling of 40-μm sections and of control (unrecorded) 200-μm sections. Additionally, morphological analyses were performed on dendrites defined by intracellular injection of biocytin into GnRH neurons from which electrophysiological recordings were obtained, with biocytin detected by peroxidase as described above. Sections were mounted, dried overnight, dehydrated in increasing concentrations of ethanol (70%–100%), cleared in xylene, and coverslipped with Permount. Biocytin- and immunocytochemically-labeled neurons were traced digitally using Neurolucida 2.1 (MicroBrightField, Inc., Colchester, VT). Morphological data obtained from each section were averaged and counted as a single observation for statistical purposes. Average cell body area, average dendrite length, and number of dendrites per cell were compared among groups by ANOVA and, if significant differences were found, between groups with a two-tailed t test. Significance was set at the $P < 0.05$ level.

Electrophysiology

Mice (21–68 days of age) were anesthetized with halothane and decapitated. The brain was quickly removed and immersed in cold (1–2 C), oxygenated (95% O_2-5% CO_2) artificial cerebrospinal fluid (ACSF) containing (in mM): NaCl (125), $NaHCO_3$ (26), NaH_2PO_4 (1.25), $MgCl_2$ (1), KCl (2.5), glucose (10), and $CaCl_2$ (3), pH 7.3–7.4. The hypothalamus was blocked with a razor blade, and 200-μm hypothalamic slices were cut in the coronal plane using a vibrating microtome (Lancer 1000). Slices were transferred to a warm incubator (32–35 C) and continuously incubated with oxygenated ACSF. Slices were incubated for at least 2 h before recording. All slices used in these studies were from the preoptic area and anterior portion of the hypothalamus, rostral to or at the level of the anterior commissure. GFP-identified and non-GFP-expressing neurons were recorded throughout this region; no regional differences have thus far been discernible in the behavior of GnRH neurons.

Patch pipettes with resistances between 2.5–5 MΩ were pulled from glass capillaries (id, 1.20 mm; od, 1.65 mm) with a Flaming Brown microelectrode puller (Sutter Instruments, Novato, CA). Pipettes were filled with a solution containing (in mM): K-gluconate (130), HEPES (10), NaCl (1), $MgCl_2$ (1), $CaCl_2$ (1), EGTA (5), biocytin (5), adenosine triphosphate (2), and brought to pH 7.2–7.4 with KOH.

For recording, slices were transferred to a chamber mounted on the stage of an upright microscope and continuously perifused with ACSF. Cells were visualized using a 40× water-immersion objective. Recording electrodes were visualized and guided to the cells of interest using an automated microdrive (Sutter MP-285). To identify GFP-expressing neurons, the slice was briefly illuminated with epifluorescence using fluorescein filters. Current-clamp recordings were obtained using an Axopatch 1D amplifier (Axon Instruments, Foster City, CA) with filtering at 5 kHz. Data were digitized on-line with a Neuro-corder (DR-484, Neurodata, Inc.) and stored on video cassettes for off-line analysis. During electrophysiological recording, cells were filled with biocytin for subsequent morphological analysis. To determine the role of voltage-dependent sodium channels in action potential firing, GFP-identified GnRH neurons were injected with 20 pA current pulses (1 Hz) in ACSF and after a 5–10 min bath application of 1 μM tetrodotoxin (TTX in ACSF; Sigma, St. Louis, MO). The effect of 1 μM TTX on spontaneous firing was also determined.

Results

Transgenic mice

Two founder animals were obtained that transmitted the GnRH-GFP transgene through the germline. In transgenic lines obtained from one of these, expression of GFP could be detected in the medial preoptic area and hypothalamus (Fig. 1A). Reproductive characteristics of this line were normal, in terms of age of vaginal opening (28 ± 2 days), onset of fertile cycles in females housed with immature males (55.8 ± 3.3 days for heterozygotes, 60.8 ± 6.4 days for homozygotes), and litter size (7.8 ± 0.6 pups, all values mean ± SEM).

Immunolabeling of GnRH peptide in fixed brain sections from transgenic mice revealed a normal distribution of GnRH-containing cell bodies and fibers from the diagonal band of Broca through the medial basal hypothalamus (Fig. 1). The majority of GnRH cell bodies were in the preoptic area just rostral to the crossing of the anterior commissure (Fig. 1A). Likewise, GnRH terminal fields in both the organum vasculosum of the lamina terminalis (Fig. 1A) and the median eminence (not shown) appeared normal. Of the several hundred GnRH neurons examined from each mouse, 84–94% could be identified by their expression of the GFP transgene. The remaining 6–16% did not express sufficiently detectable amounts of GFP (*e.g.* Fig. 1B). Although GFP was observed in the vast majority of GnRH cell bodies, its presence in processes was variable, *i.e.* considerably more GnRH-immunopositive fibers than GFP-positive fibers were visible

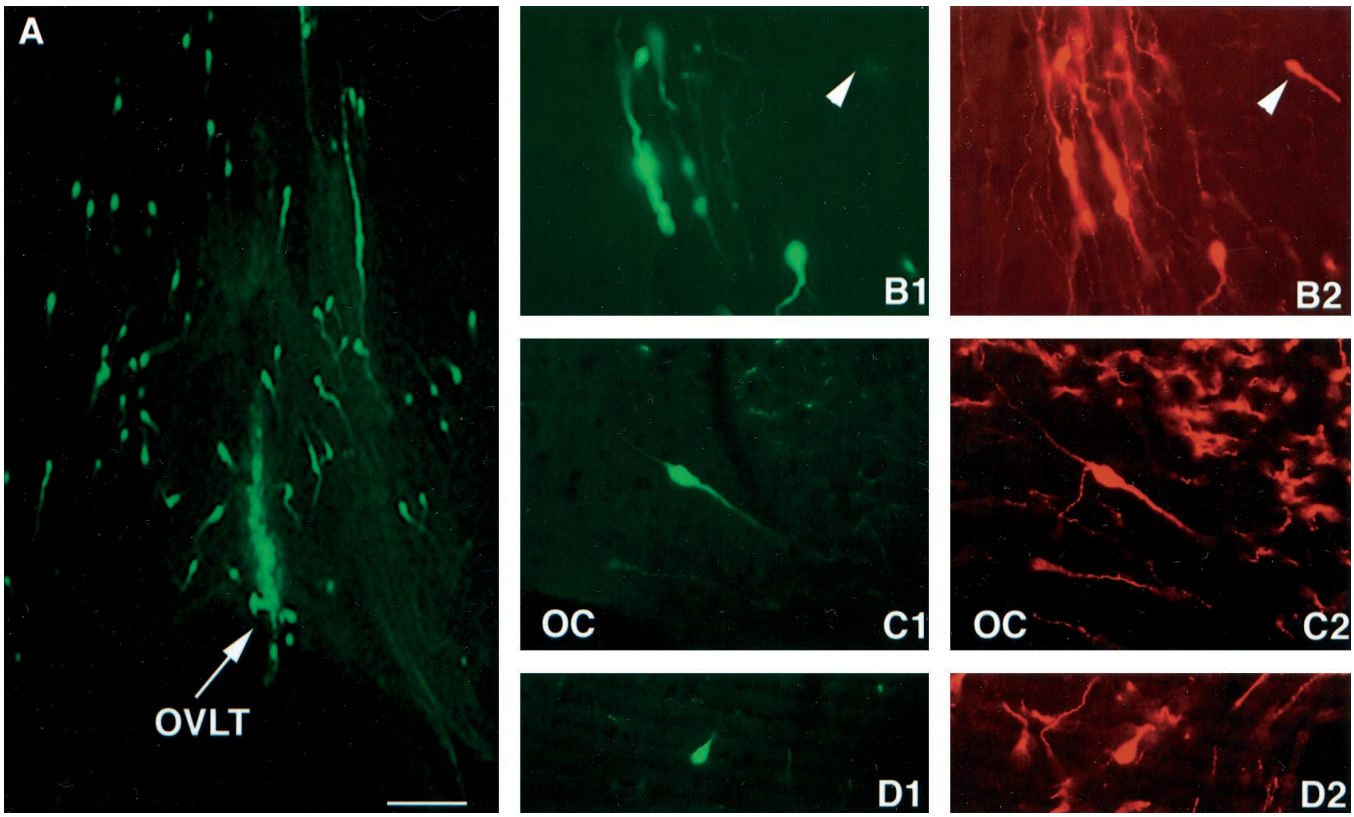

FIG. 1. Visualization of GnRH neurons with GFP. A, Section through the preoptic area of fixed 200-um section, showing multiple GnRH neurons visible through expression of GFP. GnRH neurons were detected by GFP through their normal anatomical range. B–D, Dual fluorescent imaging of GFP and GnRH labeled with Texas Red. B, Preoptic area [note GnRH-positive cell not visualized by GFP (*arrowhead*)]. C, Anterior hypothalamus over lateral optic chiasm (OC). D, Medial basal hypothalamus. In B–D, substantially more GnRH fibers are revealed by immunofluorescence than presence of GFP. *Bar* = 60 μm for A, 30 μm for B–D. OVLT, Organum vasculosum of the lamina terminalis.

(Fig. 1, B–D). Thus far, we have observed only one cell that exhibited GFP fluorescence in the absence of immunodetectable GnRH. This cell had a neuronal morphology with helical processes and beaded varicosities that are characteristic of GnRH neurons; thus, it likely represents a failure of our immunofluorescent technique, rather than ectopic expression. The fidelity of GFP identification of GnRH neurons is thus greater than 99.5% in this model system. Further, little autofluorescence was noted in brain regions containing GnRH neurons that would lead to mistaken identification of a non-GnRH neuron as a GnRH neuron. No ectopic expression of GnRH-GFP was detected in the lateral septum, basal ganglia, hippocampus, and cortex in the sections examined.

In living 200-μm hypothalamic slices, GFP-containing GnRH neurons were readily distinguishable from non-GFP-containing cells. In these slices, GFP was present throughout the full extent of the perikarya, allowing the clear delineation of cell boundaries, an important issue for sighted patch-clamp recording. Enhanced-GFP is modified to have greater expression and stability in mammalian cells. This has resulted in greater amounts of protein and hence greater visibility of cells expressing GFP for longer durations (14). In our model, this provided adequate time for cell localization, establishment of the whole-cell recording configuration and multiple recording attempts from GnRH neurons in the same slice. Following electrophysiological recording, slices were fixed and the identity of the recorded cell confirmed by detection of biocytin. In addition, the peptide phenotype of the cell was determined by immunofluorescence for GnRH. Cells which were identified by the GFP signal in slices and confirmed as recorded with biocytin were invariably immunopositive for GnRH (Fig. 2, n = 18).

GnRH neuronal morphology

Morphology of GnRH neurons was assessed in cells that were filled with biocytin during electrical recordings (200 μm). For comparison, 200-μm unrecorded sections were prepared in an identical manner and stained for GnRH peptide using standard immunoperoxidase. Morphology of neurons in these 200-μm sections was compared with that of neurons in thinner 40-μm sections stained for GnRH peptide with immunoperoxidase. Cell tracings were quantified from 21 40-μm sections (average 12.9 cells examined/section), 16 200-μm immunoperoxidase sections (average 14.5 cells examined/section), and 18 biocytin-labeled neurons in 12 200-μm directly-labeled sections (average 1.5 cells examined/section). Representative examples of a biocytin-labeled GnRH neuron (A) and immunolabeled GnRH neurons in either 200-μm (B) or 40-μm sections (C) are shown in Fig. 3. No difference was observed in cell body area using these 3 methods (Table 1). Intracellular labeling with biocytin revealed a modestly increased, but significantly higher, number of dendrites on GnRH neurons than found in immuno-

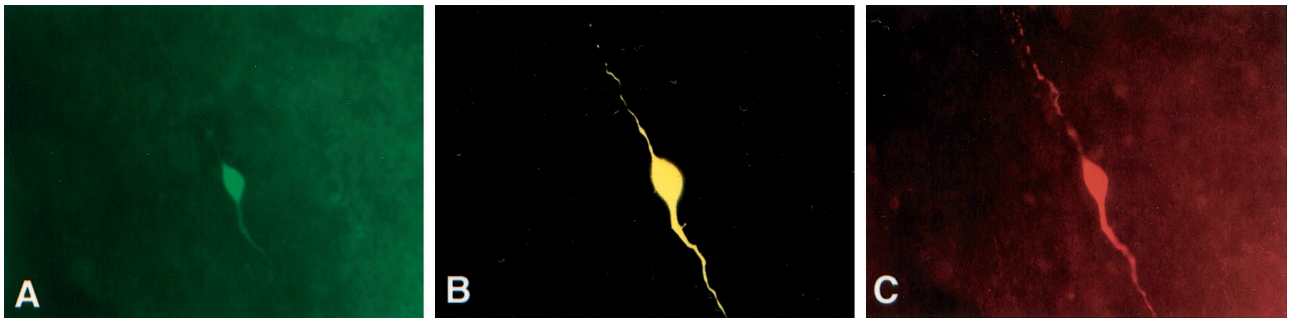

FIG. 2. Triple label of recorded GnRH neuron. A, GFP signal (*green*) used to guide patch pipette. B, Biocytin detected with streptavidin-CY3 (*yellow*), identifying recorded cell. C, Immunodetection of GnRH with CY5-conjugated secondary antibody (*red*).

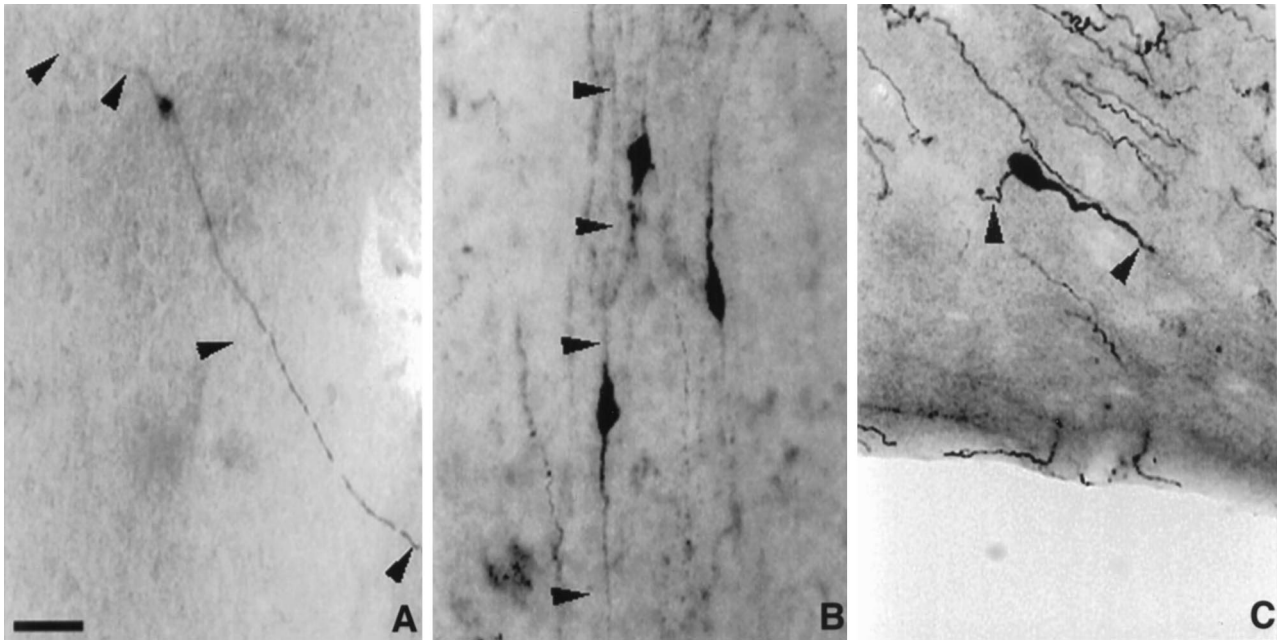

FIG. 3. Morphology of GnRH neurons labeled directly by biocytin injection followed by avidin-biotin-horseradish peroxidase reaction in 200-μm preoptic slices (*left*). Morphology of GnRH neurons labeled indirectly using immunoperoxidase methods on 200-μM slices (*center*) and 40-μm slices (*right*). *Arrowheads* indicate dendritic pathways traced for measurements shown in Table 1. *Bar*, 20 μm.

TABLE 1. Morphological characteristics of GnRH neurons labeled intracellularly with biocytin (200-μm sections) and labeled immunocytochemically (200-μm and 40-μm sections)

	Cell body area (μm^2)	Mean dendritic length (μm)	Number of dendrites per cell
200-μm (biocytin)	89.80 ± 11.04	124.81 ± 35.55[a]	2.38 ± 0.12[b]
200-μm (immuno)	85.80 ± 1.61	101.68 ± 4.7[a]	1.88 ± 0.17
40-μm (immuno)	99.56 ± 3.05	62.37 ± 4.45	1.69 ± 0.07

[a] $P < 0.05$ *vs.* 40 μm immunolabeling.
[b] $P < 0.05$ *vs.* all immunolabeling.

labeled material (Table 1). In addition, differences were observed in mean dendritic length of intracellularly labeled (biocytin) GnRH neurons. The majority of this difference in length, however, could be accounted for by the difference in section thickness, because dendritic length in 200-μm immunoperoxidase labeled sections was similar to that of directly labeled cells. The longest 2 processes measured from biocytin-labeled GnRH neurons were 436.3 and 272.3 μm. In contrast, the longest processes from immunolabeled material were 119.2 and 83.3 μm in 40-μm sections and 138.8 and 124.8 μm in 200-μm sections. This suggests that direct labeling can reveal longer dendrites than immunoperoxidase in 200-μm sections; but in the plane of section available for work, this difference was not significant. Despite an increased number of dendritic processes, biocytin-filled GnRH neurons displayed the previously described simple morphology, with few dendrites and little or no secondary branching (Refs. 17–19; Figs. 2 and 3).

Electrophysiology

Whole-cell current-clamp recording of GFP-identified GnRH neurons revealed an average resting membrane potential of approximately −65 mV (range, −51 to −89 mV; n = 23; Table 2), which was not different from non-GFP-expressing neurons (range, −79 to −50 mV; n = 18). Likewise, input resistance, an index of cell integrity, was not different between GnRH (*i.e.* GFP positive) and non-GFP-positive neurons (1.60 ± 0.16 *vs.* 1.52 ± 0.25 GΩ, Table 2). All GnRH neurons studied fired spontaneous action potentials with an amplitude of >60 mV (82.8 ± 4.9 *vs.* 76.9 ± 5.5 mV, Table 2).

GnRH neurons did not, however, fire continuously. Most current-clamp recordings from GFP-identified GnRH neurons revealed quiescent neurons with intermittent action potentials (Fig. 4). Application of 1 μM TTX, which blocks voltage-dependent sodium channels, completely eliminated spontaneous action potentials (Fig. 5A). Further, in control medium (ACSF), GnRH neurons fired repeated action potentials in response to depolarizing current injection, whereas 1 μM TTX blocked induction of action potentials in GnRH neurons by current injection (Fig. 5B).

TABLE 2. Electrophysiological characteristics of GFP-identified GnRH neurons and non-GFP-containing neurons. Values are expressed as mean ± SEM. No significant differences were observed between groups

	Resting potential (mV)	Spike amplitude (mV)	Input resistance (GΩ)
GnRH (GFP+)	67.6 ± 2.1 n = 23	82.8 ± 4.9 n = 18	1.60 ± 0.16 n = 6
Non-GnRH (GFP−)	−68.2 ± 2.1 n = 18	76.9 ± 5.5 n = 13	1.52 ± 0.25 n = 5

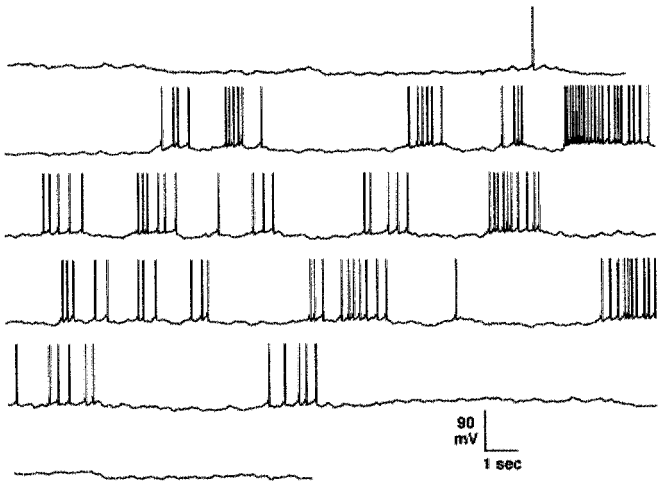

FIG. 4. GFP-identified GnRH neurons fire spontaneous action potentials (current-clamp recording). Initial resting potential in this cell was −70 mV. The cell depolarized to −55 mV and began to fire at −42 mV. The cell then returned to a resting potential of −63 mV. Maximum observed firing frequency for this cell was 4 Hz.

Discussion

Identification and study of living GnRH neurons have been complicated by their sparse distribution throughout the brain regions where they reside. By genetically targeting expression of the endogenously fluorescent protein GFP to GnRH neurons, we have generated an animal model that will make numerous experimental approaches, previously considered untenable, possible in GnRH neurons. Using this model, GnRH neurons were visualized from the diagonal band of Broca through the medial preoptic, anterior, and medial basal hypothalamus, with essentially a complete absence of ectopic expression. The fidelity of transgene expression in the present study is similar to another report of GnRH-GFP transgenics (20). This seems to differ from other GnRH promoter transgenics in which expression of the β-galactosidase gene in adult mice was evident in non-GnRH peptide-containing cells (21).

Ours is the second report of transgenic mice in which GFP has been targeted to GnRH neurons. The data we present here support those of Spergel and co-workers (20) but also extend and differ from this previous report in several important ways. First, the form of GFP used in the present study, enhanced GFP, has been demonstrated to be synthesized at higher levels in mammalian systems and thus produces a brighter and longer-lasting fluorescent signal than the form used previously (14, 22). This is likely attributable both to a mutation in enhanced GFP (rendering it more stable at the body temperature of the mouse) and to the greater extinction coefficient of enhanced GFP (14). Although direct comparisons have not been made between these mice, the

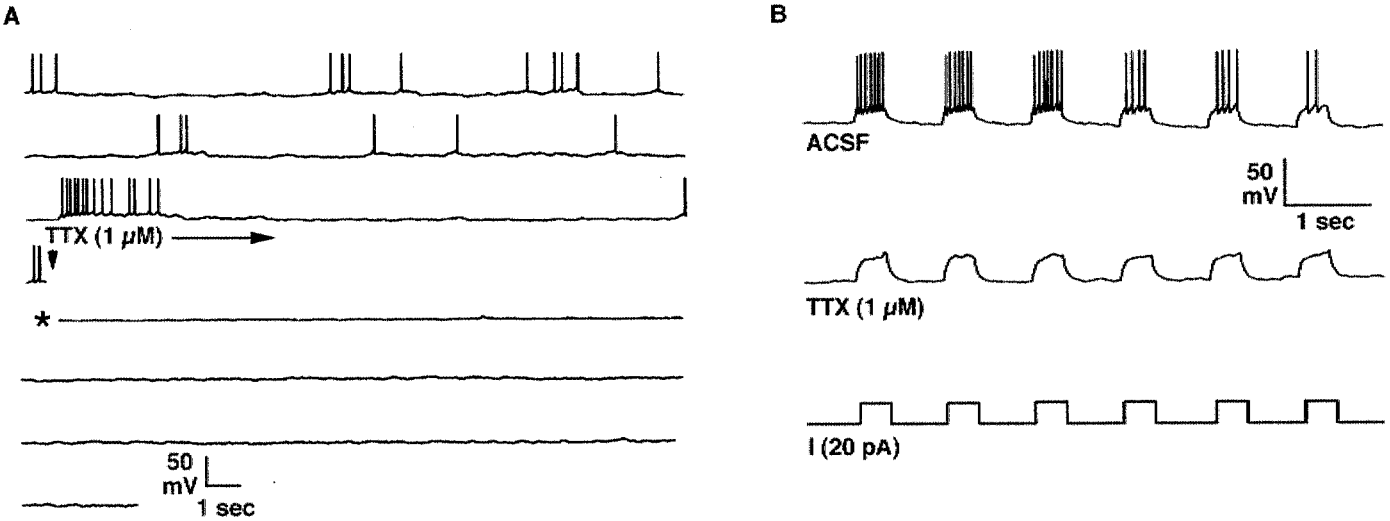

FIG. 5. TTX blockade of spontaneous (A) and current-induced (B) action potentials. A, Spontaneous action potential firing was blocked by the addition of 1 μM TTX to the bath. The *asterisk* marks resumption of record after 5-min wash-in. B, Injection of depolarizing current (20 pA, 1 Hz) induced action potential firing in GnRH neurons in artificial cerebrospinal fluid (ACSF, *top*) but not in 1 μM TTX (*middle*). The current-injection regimen is shown on the *bottom*.

remarkably stable and bright GFP signal in our mice makes identification and subsequent manipulations of identified cells straightforward. Second, our animals are the first GnRH-GFP mice for which the reproductive characteristics have been reported. This is a critical point, because the goal of this model is to study the function of GnRH neurons. If GnRH neurons were compromised by expression of the transgene, the fertility of the animals should be less than normal. Despite the advantage of being able to identify GnRH neurons with GFP, if these neurons are not functioning normally, one must call into question the properties derived from these cells. The normal reproductive parameters observed in our GnRH-GFP transgenic line attest to the proper functioning of GnRH neurons in which GFP is expressed. A third difference is that all of the cells in the present report were studied in whole-cell mode. Although Spergel and co-workers performed some whole-cell recordings, most of their findings were from nucleated patches, pulled from GnRH cell bodies and removed from the slice to be studied independently. This is a common way of examining the pharmacological properties of cell membranes. Our primary interest, however, is the function of the GnRH neurons *in situ*. Our goal, therefore, was to use an approach that provides the best opportunity to study the characteristics of individual GnRH neurons in as physiological a setting as possible, the hypothalamic slice.

Identification of living GnRH neurons in hypothalamic slice preparations offers different approaches than can be taken using existing model systems for studying GnRH neurons. The GT1 and GN cell lines, developed by genetically targeted tumorigenesis (23, 24), have been very useful particularly for biochemical approaches (reviewed in Ref. 25), while having the further advantage of studying GnRH-derived cells in the absence of other cell types. Despite their utility, the GT1 and GN model systems have some limitations. First, studies of developmental changes are precluded using these models because they seem to maintain characteristics of immature GnRH neurons (26, 27). Second, the ongoing expression of the Simian virus 40 tumor antigen may interfere with some differentiated functions. For example, GnRH neurons expressing tumor antigen are unable to target axons to the external layer of the median eminence as normal GnRH neurons do (28). Third, study of mediators that affect the afferent inputs to the GnRH neuron, such as from steroid-receptor-containing neurons, cannot be accomplished in a clonal cell line. Fourth, because of their clonal nature, GT1 and GN cell studies represent the behavior of one GnRH neuron. Thus, if (as hypothesized; reviewed in Ref. 29) subpopulations of GnRH neurons serve different functions, such as the episodic and surge modes of release, this could not be delineated with these model systems.

These limitations are avoided or minimized in the GFP-identified cell, because multiple nontransformed GnRH neurons can be studied in their local environment from animals at different ages. Because most GnRH neurons can be identified through the GFP signal, experiments to determine whether different subpopulations exist are possible. The GnRH-GFP mouse is limited, however, as a model system for biochemical investigations of the type facilitated by the GT1 and GN cell lines. In this regard, approaches such as single-cell RT-PCR and protein methodologies in GFP-identified GnRH neurons are being developed. Further, application of fluorescent-activated cell-sorting to enrich the GnRH-GFP neuronal population in primary cultures may assist with these approaches (14, 30).

We have begun to characterize the GnRH-GFP transgenic model system in two ways: morphologically and electrophysiologically. Morphological analyses of GnRH neurons thus far have relied on immunoperoxidase labeling. Direct filling of these neurons with biocytin should provide a more accurate picture of neuronal morphology, because immunoperoxidase relies on the presence of the peptide antigen for delineation of cell boundaries. Thus, areas of the neuron that exclude GnRH or contain low levels of the peptide (such as, for example, dendrites) may not be visualized. Our data are both the first characterization of GnRH neuronal morphology based on direct, intracellular labeling with biocytin and the first comparison of these different labeling techniques within a population of neurosecretory neurons with a defined peptide phenotype. When labeled with intracellular biocytin, a small, but significantly greater, number of dendrites per cell was evident than in immunolabeled material, although the well-documented simple morphology of GnRH neurons was observed. Directly labeled GnRH neurons had processes that were, on average, double the length of those of immunolabeled material from standard-thickness sections (40 μm). A substantial portion of this difference in dendrite length may be accounted for by the thickness of the section, because the average dendrite length of immunolabeled GnRH neurons in 200-μm sections was comparable with that of directly labeled cells. Although the ability to track a dendrite over greater distances is, in part, attributable to the thicker sections, it should be noted that the longest dendrites traced from directly labeled neurons were three to four times the length of immunolabeled material of the same thickness. Previous studies of immunoperoxidase-labeled material in rats (31), sheep (32), and hamster (33) indicate that GnRH neurons receive little synaptic input. The present data in biocytin-labeled neurons suggest a more extensive neurobiological substrate for synaptic impingement. It is unclear, however, whether synaptic input at such extended distances from the cell body would impact on neuronal firing because of electrotonic decay.

With regard to function, live hypothalamic slices derived from GnRH-GFP transgenic mice provide an excellent model for studying single GnRH neuronal physiology. Patch-clamp studies of GFP-identified GnRH neurons in hypothalamic slices revealed spontaneous action potentials with amplitudes (>60 mV) consistent with those of other hypothalamic neurons (33). Likewise, resting potentials in these neurons were comparable with those for nonfluorescent neurons in the same slice (−75 to −50 mV) and were within the physiological range previously reported for preoptic area neurons (34, 35) and other hypothalamic neurosecretory cells in the arcuate, supraoptic, and paraventricular nuclei (36–38). These findings suggest neither expression of GFP in GnRH neurons nor the illumination required to identify them adversely affects their viability. Study of GFP-containing GnRH neurons and non-GFP-expressing GnRH neurons would be most useful for comparison of the presently observed elec-

trophysiological characteristics, but such recordings are exceedingly difficult to obtain. This consideration notwithstanding, the GnRH neurons identified by GFP expression seem to be similar to other neurons in the hypothalamus.

In the present study, spontaneous action potentials in GnRH neurons, as well as those initiated in response to depolarizing current injection, were eliminated in the presence of tetrodotoxin. These data indicate that action potential firing in GnRH neurons involves sodium influx through TTX-sensitive voltage-gated channels. Similar results have been obtained in GT1–7 cells. Interestingly, these model GnRH neurons also express calcium-dependent action potentials mediated by low voltage-activated and high voltage-activated calcium channels (39). In GnRH neurons derived from the olfactory placode, however, more limited expression of such calcium-dependent currents was detected (40). Further work is required to reconcile these findings and to determine the role of voltage-activated calcium channels in hypothalamic GnRH neurons.

The pattern of firing observed in thin-slice preparations is different from that observed in two different models of cultured GnRH neurons. GFP-identified GnRH neurons in the present study did not fire continuously. Similar findings were reported in another GnRH-GFP mouse model using the hypothalamic thin-slice preparation (20). In contrast, cells in two different cultured preparations fired continuously, with only brief intervals (*i.e.* 10–20 sec) or complete absence of quiescence (39, 40). Of interest in this regard, pacemaker neurons from lobster stomatogastric ganglion in the intact ganglion exhibit brief episodic firing or fire action potentials when depolarized by their normal inputs (41). In contrast, after 3–4 days in culture, most of these neurons fire bursts of action potentials not seen in the intact ganglion. It is possible that similar changes in electrophysiological characteristics are induced in cultured GnRH neurons. If this were the case, cultured GnRH neurons may not accurately reflect all firing properties of hypothalamic GnRH neurons.

Our understanding of putative mechanisms linking electrophysiological activity and GnRH release is minimal. Whole-animal experiments have demonstrated GnRH release is episodic (1–5). Further, pulsatile LH release is well correlated with extracellular electrical discharges (volleys of multiunit activity) within the arcuate region of the hypothalamus (42–44). The model system we describe here will allow investigations of whether or not the pattern of action potential firing at the single GnRH neuron level reflects the intervals between multiunit activity, GnRH, and LH events. In summary, the GnRH-GFP transgenic mouse provides a model system for the high-fidelity identification and study of GnRH neurons. Use of this model in tandem with contemporary electrophysiological and biochemical approaches will greatly enhance our ability to investigate and understand this critical neuroendocrine system.

Acknowledgments

We would like to thank Dr. James Roberts for the GnRH promoter; Dr. Robert Benoit for the LR1 antibody; Kathy Dunn, Audrey Martin, and Greg Moon for expert animal care; and the Transgenic Mouse Core of the University of Virginia (P30-CA44579). The authors also thank Drs. Day, Evans, Marshall, Nunemaker, Pitts, Shupnik, and Sullivan for editorial comments; and Mr. Ron Pace for technical assistance.

References

1. **Moenter SM, Brand RM, Midgely AR, Karsch FJ** 1992 Dynamics of GnRH secretion during a pulse. Endocrinology 130:503–510
2. **Moenter SM, Caraty A, Locatelli A, Karsch FJ** 1991 Pattern of GnRH secretion leading up to ovulation in the ewe: existence of a preovulatory GnRH surge. Endocrinology 129:1175–1182
3. **Clarke IJ, Cummins JT** 1982 The temporal relationship between gonadotropin releasing hormone (GnRH) and luteinizing hormone (LH) secretion in ovariectomized ewes. Endocrinology 111:1737–1739
4. **Levine JE, Norman RL, Gliessman PM, Oyama TT, Bangsberg DR, Spies HG** 1985 *In vivo* gonadotropin-releasing hormone release and serum luteinizing hormone measurements in ovariectomized, estrogen-treated macaques. Endocrinology 117:711–721
5. **Levine JE, Ramirez VD** 1982 Luteinizing hormone-releasing hormone release during the rat estrous cycle and after ovariectomy as estimated with push-pull cannulae. Endocrinology 111:1439–1448
6. **Battaglia DF, Brown ME, Krasa HB, Thrun LA, Viguie C, Karsch FJ** 1998 Systemic challenge with endotoxin stimulates corticotropin-releasing hormone and arginine vasopressin secretion into hypophyseal portal blood: coincidence with gonadotropin-releasing hormone suppression. Endocrinology 139:4175–4181
7. **Schreihofer DA, Parfitt DB, Cameron JL** 1993 Suppression of luteinizing hormone secretion during short-term fasting in male rhesus monkeys: the role of metabolic versus stress signals. Endocrinology 132:1881–1889
8. **Foster DL, Olster DH** 1985 Effect of restricted nutrition on puberty in the lamb, patterns of luteinizing hormone (LH) secretion and competency of the LH surge system. Endocrinology 116:375–381
9. **Barrell GK, Moenter SM, Caraty A, Karsch FJ** 1992 Seasonal changes in gonadotropin-releasing hormone secretion in the ewe. Biol Reprod 46:1130–1135
10. **Karsch FJ, Dahl GE, Evans NP, Manning JM, Mayfield KP, Moenter SM, Foster DL** 1993 Seasonal changes in gonadotropin-releasing hormone secretion in the ewe: alteration in response to the negative feedback action of estradiol. Biol Reprod 49:1377–1383
11. **Silverman AJ** 1988 The gonadotropin-releasing hormone (GnRH) neuronal systems: immunocytochemistry. In: Knobil E, Neill JD (eds) The Physiology of Reproduction. Raven Press, Ltd, New York, pp 1283–1304
12. **Prasher DC, Eckenrode VK, Ward WW, Prendergast FG, Cormier MJ** 1992 Primary structure of the Aequorea victoria green-fluorescent protein. Gene 111:229–233
13. **Chalfie M, Tu Y, Euskirchen G, Ward WW, Prasher DC** 1994 Green fluorescent protein as a marker for gene expression. Science 263:802–805
14. **Cormack BP, Valdivia RH, Falkow S** 1996 FACS-optimized mutants of the green fluorescent protein (GFP). Gene 173:33–38
15. **Hogan (ed)** 1994 Manipulating the Mouse Embryo, 2nd ed. Cold Spring Harbor Laboratory Press, Plainview, NY
16. **Moenter SM, Karsch FJ, Lehman MN** 1993 Fos expression during the estradiol-induced GnRH surge of the ewe: induction in GnRH and other neurons. Endocrinology 133:896–903
17. **Lehman MN, Robinson JE, Karsch FJ, Silverman AJ** 1986 Immunocytochemical localization of luteinizing hormone-releasing hormone (LHRH) pathways in the sheep brain during anestrus and the mid-luteal phase of the estrous cycle. J Comp Neurol 244:19–35
18. **Silverman AJ, Antunes JL, Abrams GM, Nilaver G, Thau R, Robinson JA, Ferin M, Crey LC** 1982 The luteinizing hormone releasing hormone pathways in rhesus (Macaca mulatta) and pig-tailed (Macaca nemestrina) monkeys: new observations on thick, unembedded sections. J Comp Neurol 211:309–317
19. **Witkin JW, Paden CM, Silverman AJ** 1982 The luteinizing hormone-releasing hormone (LHRH) systems in the rat brain. Neuroendocrinology 35:429–438
20. **Spergel DJ, Krüth U, Haneley DF, Sprengel R, Seeburgh PH** 1999 GABA- and glutamate-activated channels in green fluorescent protein-tagged gonadotropin-releasing hormone neurons in transgenic mice. J Neurosci 19:2037–2050
21. **Skynner MJ, Slater R, Sim JA, Allen ND, Herbison AE** 1999 Promoter transgenics reveal multiple gonadotropin-releasing hormone-I-expressing cell population of different embryological origin in mouse brain. J Neurosci 19:5955–5966
22. **Zolotukhin S, Potter M, Hauswirth WW, Guy J, Muzyczka N** 1996 A "humanized" green fluorescent protein cDNA adapted for high-level expression in mammalian cells. J Virol 70:4646–4654
23. **Mellon PL, Windle JJ, Goldsmith PC, Padula CA, Roberts JL, Weiner RI** 1990 Immortalization of hypothalamic GnRH neurons by genetically targeted tumorigenesis. Neuron 5:1–10
24. **Radovick S, Wray S, Lee E, Nicols DK, Nakayama Y, Weintraub BD, Westphal H, Cutler Jr GB, Wondisford FE** 1991 Migratory arrest of gonadotropin-releasing hormone neurons in transgenic mice. Proc Natl Acad Sci USA 88:3402–3406
25. **Moenter SM, Weiner RI** 1995 The use of clonal neuronal cell lines as tools to

understand neuroendocrine systems and mechanisms regulating pulsatile secretion of neuropeptides. Curr Opin Endocrinol Metab 2:181–185
26. **Longo KM, Sun Y, Gore AC** 1998 Insulin-like growth factor-I effects on gonadotropin-releasing hormone biosynthesis in GT1–7 cells. Endocrinology 139:1125–1132
27. **Allen MP, Zeng C, Schneider K, Xiong X, Meintzer MK, Bellosta P, Basilico C, Varnum B, Heidenreich KA, Wierman ME** 1999 Growth arrest-specific gene 6 (Gas6)/adhesion related kinase (Ark) signaling promotes gonadotropin-releasing hormone neuronal survival via extracellular signal-regulated kinase (ERK) and Akt. Mol Endocrinol 13:191–201
28. **Weiner RI, Thind KK, Windle JJ, Padula CA, Mellon P, Goldsmith PC** 1991 Expression of SV-40 T-antigen in GnRH neurons inhibits the organization of terminals in the median eminence. Soc Neurosci Abstr 17:183 (Abstract)
29. **Kimura F, Funabashi T** 1998 Two subgroups of gonadotropin -releasing hormone neurons control gonadotropin secretion in rats. News Physiol Sci 13:225–231
30. **Galbraith DW, Anderson MT, Herzenberg LA** 1999 Flow cytometric analysis and FACS sorting of cells based on GFP accumulation. Methods Cell Biol 58:315–341
31. **Witkin JW, Silverman AJ** 1985 Synaptology of luteinizing hormone-releasing hormone neurons in the rat preoptic area. Peptides 6:263–271
32. **Lehman MN, Karsch FJ, Robinson JE, Silverman AJ** 1988 Ultrastructure and synaptic organization of luteinizing hormone-releasing hormone (LHRH) neurons in the anestrous ewe. J Comp Neurol 273:447–458
33. **Lehman MN, Silverman AJ** 1988 Ultrastructure of luteinizing hormone-releasing hormone (LHRH) neurons and their projections in the golden hamster. Brain Res Bull 20:211–221
34. **Hoffman NW, Kim YI, Gorski RA, Dudek FE** 1994 Homogeneity of intracellular electrophysiological properties in different neuronal subtypes in medial preoptic slices containing the sexually dimorphic nucleus of the rat. J Comp Neurol 345:396–408
35. **Hoffman NW, Wuarin J-P, Dudek FE** 1994 Whole-cell recordings of spontaneous synaptic currents in medial preoptic neurons from rat hypothalamic slices: mediation by amino acid neurotransmitters. Brain Res 660:349–352
36. **Belousov AB, van den Pol AN** 1997 Local synaptic release of glutamate from neurons in the rat hypothalamic arcuate nucleus. J Physiol 499:747–761
37. **Wuarin JP, Dudek FE** 1993 Patch-clamp analysis of spontaneous synaptic currents in supraoptic neuroendocrine cells of the rat hypothalamus. J Neurosci 13:2323–2331.
38. **Boudaba C, Szabo K, Tasker JG** 1996 Physiological mapping of local inhibitory inputs to the hypothalamic paraventricular nucleus. J Neurosci 16:7151–7160
39. **Van Goor F, Krsmanovic LZ, Catt KJ, Stojikovic SS** 1999 Control of action potential-driven calcium influx in GT1 neurons by the activation status of sodium and calcium channels. Mol Endocrinol 13:587–603
40. **Kusano K, Gueshko S, Gainer H, Wray S** 1995 Electrical and synaptic properties of embryonic luteinizing hormone-releasing hormone neurons in explant cultures. Proc Natl Acad Sci USA 92:3918–3922
41. **Turrigiano G, Abbott LF, Marder E** 1994 Activity-dependent changes in the intrinsic properties of cultured neurons. Science 264:974–977
42. **Wilson RC, Kesner JS, Kaufman JM, Uzmura T, Akema T, Knobil E** 1984 Central electrophysiological correlates of pulsatile luteinizing hormone secretion in the rhesus monkey. Neuroendocrinology 39:256–260
43. **Tanaka T, Ozawa T, Hoshino K, Mori Y** 1995 Changes in the gonadotropin-releasing hormone pulse generator activity during the estrous cycle in the goat. Neuroendocrinology 62:553–561
44. **Hiruma H, Nishihara M, Kimura F** 1992 Hypothalamic electrical activity that relates to the pulsatile release of luteinizing hormone exhibits diurnal variation in ovariectomized rats. Brain Res 582:119–122